STATISTICS IN TRANSITION new series, December 2025

Vol. 26, No. 4, pp. xxx-xxx, https://doi.org/10.59139/stattrans-2025-xxx

Received – xx.xx.xxxx; accepted – xx.xx.xxxxx

Inverse Power Lomax Poisson distribution: properties and applications in modelling negatively-skewed reliability data

A. A. Ogunde¹, E. F. Nymphas²

Abstract

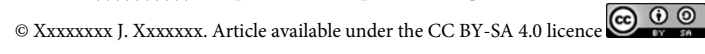
In this paper, we propose a new, four-parameter distribution with increasing, decreasing, bathtub-shaped and a unimodal failure rate, called the Inverse Power Lomax Poisson (IPLP) distribution. The new distribution combines Inverse Power Lomax (IPL) and Poisson distributions. We derive several properties of the new distribution: its probability density function, its reliability and failure rate functions, the quantiles, the stress-strength parameter, complete and incomplete moments, the moment generating function, the probability weighted moment, Rènyi and q-entropies, and order statistics. The study presents the estimation of the model's parameters based on the maximum likelihood method. The applications of the new distribution are presented using two real data sets, showing its flexibility and potential in modelling lifetime data.

Key words: probability weighted moments, incomplete moments, quantile function, Renyi entropy.

1. Introduction

The Inverse Power Lomax (IPL) distribution, introduced and developed by Hassan and Abd-Allah (2019), as a reciprocal of the Power Lomax distribution, contains distributions with bathtub-shaped and unimodal failure rates, as well as a broader class of monotone failure rates. The IPL model provides a tractable and close-form solution to many problems in reliability studies. However, it does not give a reasonably good parametric fit in some real-life applications most especially when the data is extremely skewed, Hassan and Abd-Allar (2019). However, several works have been done to develop new families of probability distributions that extend standard probability distributions while at the same time making them more flexible and tractable. Abdul-

² Corresponding author. Department of Statistics, University of Ibadan, Ibadan, Nigeria. E-mail: a.xxxxx@yyyyyyyyedu.pl. ORCID: https://orcid.org/xxxx-xxxx-xxxx.



¹ Department of Statistics, University of Ibadan, Ibadan, Nigeria. E-mail: a.xxxxx@yyyyyyyyyyyyyyyyyyyol.oRCID: https://orcid.org/xxxx-xxxx-xxxx.

Moniem and Abdel-Hameed (2012) studied the exponentiated Lomax distribution. Lemonte and Cordeiro (2013) studied the properties of beta Lomax, Kumaraswamy Lomax and McDonald developed the Lomax distributions. Cordeiro et al. (2013) introduced the gamma-Lomax model. The Weibull Lomax was proposed and studied by Tahir et al. (2015). The Gumbel-Lomax distribution was investigated by Tahir et al. (2016). The type II Topp Leone power Lomax distribution was studied by Al-Marzouki et al. (2020), Haq et al. (2020) studied the Marshal-Olkin Power Lomax distribution. The sine Power Lomax and the sine Inverse Power Lomax distribution was studied by Nagarjuma and Chesneau (2021, 2022). The Kumaraswamy generalised Inverse Lomax and the type II Topp-Leone Inverse Power Lomax distributions were proposed and studied by Ogunde et al. (2023, 2024). They developed the new model using the Kumaraswamy and type II Topp-Leone generators, respectively.

A random variable X follows the IPL distribution if its cumulative distribution function (CDF) takes the form

$$G(x; \alpha, \rho, \lambda) = \left(1 + \frac{x^{-\alpha}}{\lambda}\right)^{-\rho}, \ x > 0; \ \alpha, \rho, \lambda > 0$$
 (1)

The corresponding probability density function (PDF) is

$$g(x; \alpha, \rho, \lambda) = \frac{\alpha \rho}{\lambda} x^{-\alpha - 1} \left(1 + \frac{x^{-\alpha}}{\lambda} \right)^{-\rho - 1}, \quad x > 0; \quad \alpha, \rho, \lambda > 0$$
 (2)

The survival and hazard rate functions of the IPL distribution are, respectively,

$$S(x; \alpha, \rho, \lambda) = 1 - G(x; \alpha, \rho, \lambda) = 1 - \left(1 + \frac{x^{-\alpha}}{\lambda}\right)^{-\rho}, \tag{3}$$

and

$$h(x;\alpha,\rho,\lambda) = \frac{g(x;\alpha,\rho,\lambda)}{S(x;\alpha,\rho,\lambda)} = \frac{\alpha\rho x^{-\alpha-1} \left(1 + \frac{x^{-\alpha}}{\lambda}\right)^{-\rho-1}}{\lambda \left\{1 - \left(1 + \frac{x^{-\alpha}}{\lambda}\right)^{-\rho}\right\}}.$$
 (4)

Where α and ρ are positive shape parameters and λ is a scale parameter. In the literature, several authors proposed a new distribution to model lifetime data by combining some discrete distribution together with other known continuous distributions. Roman et al. (2012) proposed a long-term exponential geometric distribution. Recently, compounding distributions for Lomax with discrete one has been presented by some authors. For instance; the Lomax Poison distribution was proposed by Abd-Elfattah et al. (2013). Ramos et al. (2013) studied the exponentiated Lomax Poisson distribution, Al-Zahrani and Sagor (2014) developed and studied the Lomax-Logarithm distribution. Al-Zahrani (2015) and Hassan and Abd-Alla (2017) developed the extended Poisson Lomax and the exponentiated Lomax distribution, respectively. Hassan and Nassr (2018) investigated the properties of the Power Lomax Poisson distribution. Nargajuma et al. (2022) proposed and studied the Nadarajah-Haghighi Lomax distribution, among many others.

In this study, we propose and study a new four-parameter distribution, named the Inverse Power Lomax Poisson (IPLP) distribution, which contains the Inverse

Power Lomax (IPL), the Inverse Lomax Poisson (*ILP*), and the Inverse Lomax distributions as the sub-models. The chief motivation for introducing the *IPLP* distribution is that the distribution, due to its flexibility, can accommodate different forms of the shape of the hazard function. The distribution also provides a reasonable parametric fit to skewed data that cannot be properly fitted by other distributions and is a suitable model in other areas such as insurance, seismography, medicine, actuarial science, demography, reliability, and survival studies.

The paper is organized as follows. In Section 2, we developed the IPLP distribution and derived its density, survival and hazard rate, cumulative, and reversed hazard rate, and the quantile functions. Some of the properties of the IPLP distribution are given in Section 3, which includes moments, moment generating functions, incomplete moments, Renyi and q entropies, probability weighted moments, and order statistics. Estimation and real data application was demonstrated in Section 4. In Section 5, we concluded.

2. The Inverse Power Lomax Poisson distribution

Suppose that the random variable X has the IPL distribution, where its cdf and pdf are given in (1) and (2). Given N, let X_1, \ldots, X_n be independent and identify distributed random variables from IPL distribution. Suppose N is distributed according to zero truncated Poisson distribution with PDF

$$T(N=n) = \frac{e^{\zeta \zeta^n}}{n!(1-e^{-\zeta})}, \qquad n=1,2,..., \ \zeta > 0$$
 (5)

Let $T = max(X_1, ..., X_N)$, then the CDF of T/N = n is given by

$$F_{T/N=n}(t) = \left(1 + \frac{t^{-\alpha}}{\lambda}\right)^{-\rho n},\tag{6}$$

which is the Exponentiated Inverse Power Lomax distribution with parameters ρn , α and λ . The *IPLP* distribution, represented by *IPLP*(α , λ , ρ , ζ), is defined by the marginal *CDF* of T, i.e.

$$F(x;\alpha,\rho,\lambda,\zeta) = \frac{1 - e^{-\zeta \left(1 + \frac{x^{-\alpha}}{\lambda}\right)^{-\rho}}}{-e^{-\zeta} + 1},\tag{7}$$

This newly developed distribution contains the Inverse Lomax and the Inverse Lomax Poisson distribution. The pdf of the *IPLP* distribution is given by

$$f(x; \alpha, \rho, \lambda, \zeta) = \frac{\alpha \rho \zeta x^{-\alpha - 1} \left(1 + \frac{x^{-\alpha}}{\lambda}\right)^{-\rho - 1} \left\{ e^{-\zeta \left(1 + \frac{x^{-\alpha}}{\lambda}\right)^{-\rho}} \right\}}{\lambda (-e^{-\zeta} + 1)},$$
(8)

where α , ρ , ζ are positive shape parameters and λ is a positive scale parameter. The reliability (R(x)) and hazard rate ((h(x)) functions, reversed hazard and cumulative hazard functions of the *IPLP* distribution are, respectively, given by

$$R(x;\alpha,\rho,\lambda,\zeta) = 1 - \frac{1 - e^{-\zeta\left(1 + \frac{t^{-\alpha}}{\lambda}\right)^{-\rho}}}{-e^{-\zeta} + 1} = \frac{e^{-\zeta\left(1 + \frac{t^{-\alpha}}{\lambda}\right)^{-\rho}} - e^{-\zeta}}{-e^{-\zeta} + 1},\tag{9}$$

$$h(x;\alpha,\rho,\lambda,\zeta) = \frac{\alpha\rho\zeta x^{-\alpha-1} \left(1 + \frac{x^{-\alpha}}{\lambda}\right)^{-\rho-1} e^{-\zeta\left(1 + \frac{x^{-\alpha}}{\lambda}\right)^{-\rho}}}{\lambda e^{-\zeta\left\{e^{-\zeta\left(1 + \frac{x^{-\alpha}}{\lambda}\right)^{-\rho}} - 1\right\}}},$$
(10)

$$\varphi(x;\alpha,\rho,\lambda,\zeta) = \frac{\alpha\rho\zeta x^{-\alpha-1} \left(1 + \frac{x^{-\alpha}}{\lambda}\right)^{-\rho-1} e^{-\zeta\left(1 + \frac{x^{-\alpha}}{\lambda}\right)^{-\rho}}}{\lambda\left\{1 - e^{-\zeta\left(1 + \frac{x^{-\alpha}}{\lambda}\right)^{-\rho}}\right\}},$$
(11)

and

$$H = \log\left(1 - e^{-\zeta\left(1 + \frac{\chi - \alpha}{\lambda}\right)^{-\rho}}\right) - \log\left(-e^{-\zeta} + 1\right). \tag{12}$$

The plots of distribution, density and hazard rate functions of the *IPLP* distribution for different values of $(\alpha, \rho, \zeta, \lambda)$ are given in Figures 1, 2 and 3, respectively.

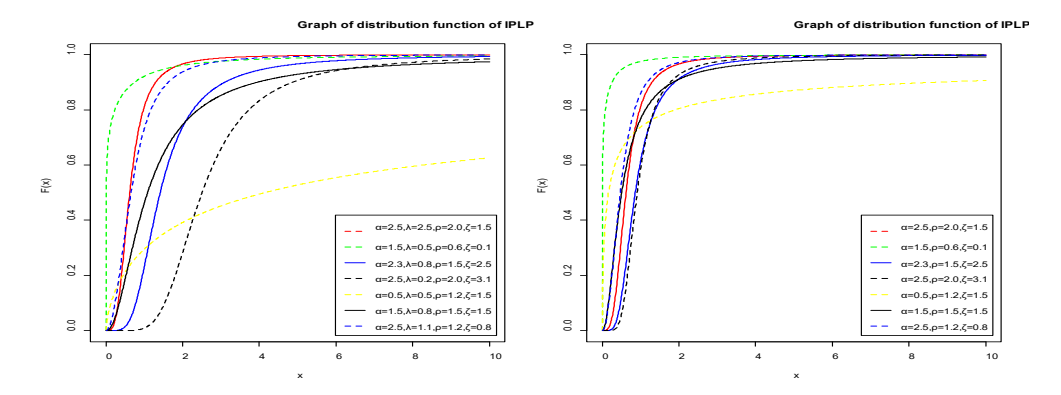


Figure 1. Graph of distribution function of IPLP distribution

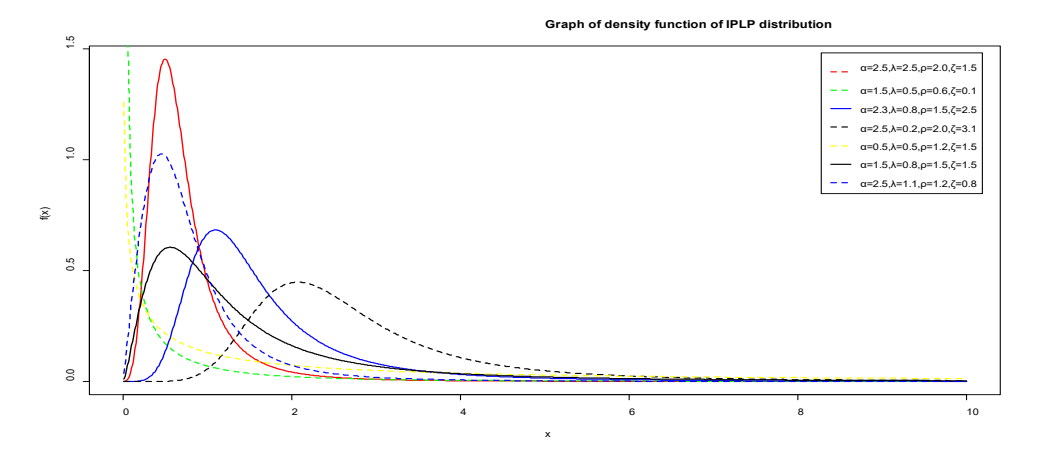


Figure 2. Graph of density function of IPLP distribution

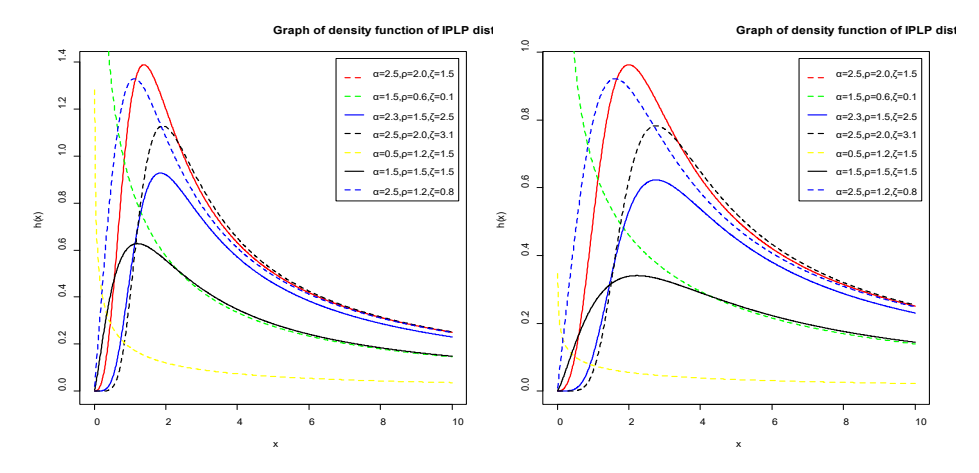


Figure 3. Graph of hazard function of *IPLP* distribution

From Figure 3, it can be observed that the hazard rate function of the *IPLP* model exhibits decreasing, increasing, reversed bathtub, and reversed J-shape curves. This indicates that the *IPLP* distribution can be used effectively to model skewed data exhibiting various shapes of the hazard function.

2.1. Quantiles of the IPLP distribution

The quantile function can be used in the study of some important features and characteristics of a distribution which includes dispersion, skewness and kurtosis. Also, the quantiles of a distribution can be employed in data generation from a distribution. The k^{th} quantile of the *IPLP* distribution is given by

$$x_k = \left\{ \lambda \left[\left(-\frac{1}{\zeta} \ln[1 + (1 - k)(-e^{-\zeta} + 1)] \right)^{-1/\rho} - 1 \right] \right\}^{-1/\alpha}, \tag{13}$$

which is used for data generation from the *IPLP* distribution. The median (middle quartile) and the upper quartiles of the *IPLP* distribution can be obtained by taking k = 0.5 and 0.75 respectively.

2.2. Mixture representation of *IPLP* model

Using the binomial series expansion given by

$$e^z = \sum_{p=0}^{\infty} \frac{z^p}{p!},\tag{14}$$

the mixture representation of *IPLP* model is given by

$$f(x;\alpha,\rho,\lambda,\zeta) = \frac{\alpha\rho\zeta}{\lambda} \sum_{m=0}^{\infty} \frac{1}{m!(e^{\zeta}-1)} x^{-\alpha-1} \left(1 + \frac{x^{-\alpha}}{\lambda}\right)^{-[\rho(m+1)+1]}.$$
 (15)

The expression given in (15) can be described as the Exponentiated Inverse Power distribution with scale parameter λ and shape parameters α and $\rho(m+1)$.

3. Statistical Properties of *IPLP* distribution

The following properties of the IPLP model are investigated.

3.1. Moments of IPLP distribution

The r^{th} moments of the *IPLP* distribution can be expressed as

$$\mu_r' = E(X^r) = \int_{-\infty}^{\infty} x^r f(x; \alpha, \rho, \lambda, \zeta) dx$$
 (16)

Using (15) in (16) we get

$$\mu_r' = \frac{\alpha\rho\zeta}{\lambda} \sum_{m=0}^{\infty} \frac{1}{m!(e^{\zeta} - 1)} \int_{-\infty}^{\infty} x^{r - \alpha - 1} \left(1 + \frac{x^{-\alpha}}{\lambda} \right)^{-[\rho(m+1) + 1]} dx \tag{17}$$

After some algebraic manipulation, we have

$$\mu_r' = \frac{\rho \zeta}{\lambda^{r}/\alpha} \sum_{m=0}^{\infty} \frac{(-1)^m}{m!(e^{\zeta} - 1)} B[(1 - r/\alpha), (r/\alpha + \zeta(m+1))]$$
 (18)

The moment generating function of X, $M_x(t)$, is given by

$$M_{x}(t) = \int_{-\infty}^{\infty} e^{tX} f(x; \alpha, \rho, \lambda, \zeta) dx = \sum_{r=0}^{\infty} \frac{t^{r}}{r!} E(X^{r}).$$
 (19)

Using the expression given in (18) for the r^{th} moments of the *IPLP* distribution, we have

$$M_{\chi}(t) = \frac{\rho \zeta}{\lambda^{r}/\alpha} \sum_{m=0}^{\infty} \frac{t^{r}}{m! r! (e^{\zeta} - 1)} B[(1 - r/\alpha), (r/\alpha + \zeta(m+1))], \tag{20}$$

where $B(a,b) = \frac{\Gamma a \Gamma b}{\Gamma(a+b)}$. From the above expression in (20), setting r = 1,2,3,4,5, and 6, respectively, we obtain the first six moments about the origin of *IPLP* distribution.

The n^{th} central moment of X, of IPLP model, say μ_n , is given as

$$\mu_n = E(x - \mu)^n = \sum_{p=0}^{\infty} (-1)^p \binom{n}{p} \mu_r'^p \mu_{n-p}'.$$

The cumulant (κ_n) of X can be obtained as

$$\kappa_n = \mu'_n - \sum_{r=0}^{n-1} {n-1 \choose r-1} \kappa_r \mu'_{n-r}.$$

Table 1 presents the first six moments, standard deviation (σ) , coefficient of variation (CV), skewness (S_k) , and kurtosis (k_u) for various values of the parameters of *IPLP* distribution. It could be observed that as the values of the parameters increase the values of the lower moment decrease and increase for higher moments. The same is observed for skewness and kurtosis except for higher values of the parameters. This further demonstrates the flexibility of the *IPLP* model in handling data of different degree of skewness and kurtosis.

Specification	$\alpha = 7.0, \lambda = 5.5$								
Moment	$\rho = 0.5$,	$\rho = 1.2$,	$\rho = 2.5$,	$\rho = 3.5$,	$\rho = 6.5$,				
мотепі	$\zeta = 0.5$	$\zeta = 1.5$	$\zeta = 4.0$	$\zeta = 4.5$	$\zeta = 6.5$				
μ_1'	0.6525	0.8148	0.9165	0.9015	0.8988				
μ_2'	0.4776	0.7011	0.8666	0.8320	0.8161				
μ_3'	0.3899	0.6448	0.8538	0.7917	0.7498				
μ_4'	0.3600	0.6491	0.8938	0.7877	0.6989				
μ_5'	0.3944	0.7546	1.0413	0.8491	0.6661				
μ_6'	0.6062	1.2026	1.5792	1.1308	0.6703				
σ	0.2274	0.1929	0.1632	0.1389	0.0909				
CV	0.3485	0.2367	0.1781	0.1541	0.1011				
S_k	0.8988	1.8008	2.4746	2.5583	1.9237				
k_{ν}	6.9213	13.0353	20.6319	22.5148	15.7185				

Table 1. First six moments, σ , CV, S_k , and k_u for IPLP distribution

3.2. Incomplete moment of IPLP distribution

The r^{th} incomplete moments of the *IPLP* distribution is defined by

$$\varphi_r(t) = \alpha \rho \zeta \int_{-\infty}^t x^{r-\alpha-1} \frac{\left(1 + \frac{x^{-\alpha}}{\lambda}\right)^{-\rho-1} \left\{ e^{-\zeta \left(1 + \frac{x^{-\alpha}}{\lambda}\right)^{-\rho}} \right\}}{\lambda (-e^{-\zeta} + 1)} dx$$
 (21)

Using (14), we can write the expression given in (21) as

$$\varphi_r(t) = \frac{\alpha\rho\zeta}{\lambda} \sum_{m=0}^{\infty} \frac{1}{m!(e^{\zeta} - 1)} \int_{-\infty}^{t} x^{r - \alpha - 1} \left(1 + \frac{x^{-\alpha}}{\lambda} \right)^{-[\rho(m+1) + 1]} dx \tag{22}$$

After some algebraic manipulation, we have

$$\varphi_r(t) = \frac{\rho\zeta}{\lambda^{r/\alpha}} \sum_{m=0}^{\infty} \frac{1}{m!(e^{\zeta} - 1)} B\left[(1 - r/\alpha), (r/\alpha + \zeta(m+1); \frac{t^{-\alpha}}{\lambda}) \right]. \tag{23}$$

3.3. Rènyi and q-entropies of IPLP distribution

Suppose X is a random variable with continuous cumulative distribution function F(x) and probability density function f(x). Then the fundamental uncertainty measure for distribution F (named the entropy of F) is defined as I(x) = E[-log(f(X))]. Statistical entropy is a probabilistic measure of uncertainty, also a measure of a reduction in that uncertainty. Numerous entropy and information indices are considered in the literature, among them the Rényi and q entropy. The Rènyi entropy of a random variable F0 can be used to obtain the measures of uncertainty and variation of a system and it is defined ($\partial > 0$ and $\partial \neq 1$) as:

$$I_R(\partial) = \frac{1}{1-\partial} \log[M(\partial)], \tag{24}$$

where

$$M(\partial) = \int_{-\infty}^{\infty} f^{\partial}(x) dx,$$

Using

$$M(\partial) = \frac{\alpha^{\partial} \rho^{\partial} \zeta^{\partial}}{\lambda^{\partial} (-e^{-\zeta} + 1)^{\partial}} \int_{-\infty}^{\infty} x^{-\partial(\alpha + 1)} \left(1 + \frac{x^{-\alpha}}{\lambda} \right)^{-\partial(\rho + 1)} \left\{ e^{-\zeta \left(1 + \frac{x^{-\alpha}}{\lambda} \right)^{-\rho}} \right\}^{\partial} dx, \tag{25}$$

After some algebraic manipulation we have

$$M(\partial) = \frac{\alpha^{\partial} \rho^{\partial}}{\lambda^{\partial} (-e^{-\zeta} + 1)^{\partial}} \sum_{i=1}^{\infty} \frac{(-1)^{i} \zeta^{\partial + i} \partial^{i}}{i!} \int_{-\infty}^{\infty} x^{-\partial(\alpha + 1)} \left(1 + \frac{x^{-\alpha}}{\lambda} \right)^{-[\partial(\rho + 1) + \partial i]} dx, \tag{26}$$

Further simplification gives

$$M(\partial) = W^{i}B\left[\frac{\partial(\alpha+1)-1}{\alpha}, \frac{2\alpha+1-\partial(\alpha+1)-\alpha\{\rho i-\partial(\rho+1)\}}{\alpha}\right]$$
(27)

where

$$W^{i} = \frac{\alpha^{\partial - 1} \rho^{\partial} \lambda^{\frac{\partial - 1}{\alpha}}}{(-e^{-\zeta} + 1)^{\partial}} \sum_{i=1}^{\infty} \frac{(-1)^{i} \zeta^{\partial + i} \partial^{i}}{i!}.$$

Finally, we obtain an expression for the Renyi entropy of IPLP distribution as

$$I_{R}(\partial) = \frac{1}{1-\partial} log \left\{ W^{i} B \left[\frac{\partial(\alpha+1) - 1}{\alpha}, \frac{2\alpha + 1 - \partial(\alpha+1) - \alpha \{\rho i - \partial(\rho+1)\}}{\alpha} \right] \right\}, \tag{28}$$

The q-entropy, Z_q , is defined by

$$Z_q = \frac{1}{q-1} \log[1 - (q-1)M(\partial)]$$

Using $M(\partial)$, we have

$$\begin{split} Z_q &= \frac{1}{q-1} log \left[1 - (q - 1)W^i B \left[\frac{\partial (\alpha+1) - 1}{\alpha}, \frac{2\alpha+1 - \partial (\alpha+1) - \alpha \{\rho i - \partial (\rho+1)\}}{\alpha} \right] \right] \end{split}$$

3.4. Probability Weighted Moments (PWMs)

Probability weighted moments (PWMs) are defined as the expectations of certain functions of a random variable. They are only considered when the ordinary moments of the random variable exist. The PWMs method can generally be employed in estimating the parameters of a distribution whose inverse form cannot be expressed explicitly. In this paper we obtained PWMs of the IPLP distribution since they can be used for estimating the IPLP parameters. For a random variable with the pdf f(.) and cdf F(.), the PWMs function can be obtained as follows:

$$\Gamma_{p,r} = E[X^p F(X)^r] = \int_{-\infty}^{\infty} x^p \big(F(x)\big)^r f(x) dx \tag{29}$$

Putting (7) and (8) in (29), followed by algebraic manipulation, we have

$$\Gamma_{p,r} = \frac{\alpha\rho\zeta}{\lambda(-e^{-\zeta}+1)^{1+r}} \sum_{i,j=0}^{\infty} \frac{(-1)^{r+j}}{j!} {r \choose i} (1+r)^j \int_{-\infty}^{\infty} x^{\rho-\alpha-1} \left(1 + \frac{x^{-\alpha}}{\lambda}\right)^{-[\rho(i+j)+1]} \\
= \frac{\rho\zeta\lambda^{-p/\alpha}}{(-e^{-\zeta}+1)^{1+r}} \sum_{j=0}^{\infty} \frac{(-1)^{r+j}}{j!} {r \choose i} (1+r)^j \zeta^j B \left[(1-\frac{p}{\alpha}), \frac{p+\alpha[\rho(1+j)-1]}{\alpha} + 1 \right]$$

3.5. Order statistics

In real life experiment order statistics plays a very crucial and informative role in understanding the concepts of system reliability. Randomly selecting samples from *IPLP* distribution and arranging them in increasing/decreasing other of magnitude, i.e. $(T_{1:n} < T_{2:n} < \cdots < T_{n:n})$, constitute an ordered sample which can be investigated as order statistics.

3.5.1 Derivation of the j^{th} order statistics

Consider $X_{(j:n)}$ denoting the j^{th} ordered sample from the *IPLP* distribution given in (8). Then the Probability density for the j^{th} order statistics is

$$f_{j}(x_{(j)}, \Psi) = \frac{1}{B(j, n+j+1)} \left\{ G((x_{(j)}, \Psi)) \right\}^{n-1} g(x_{(j)}, \Psi) \left\{ 1 - G((x_{(j)}, \Psi)) \right\}^{n-j}$$
(31)

where $\Psi = (\alpha, \rho, \zeta, \lambda)$. Further simplification using Taylor series expansion gives

$$f_j(x_{(j)}, \Psi) = \frac{1}{B(j, n+j+1)} \sum_{i=0}^{\infty} (-1)^i {n-j \choose i} \left\{ G((x_{(j)}, \Psi)) \right\}^{n+i-1} g(x_{(j)}, \Psi)$$
(32)

Inserting (7) and (8) in (32) followed by further simplification using Taylor series, we have

$$f_{j}(x_{(j)}, \Psi) = \frac{\alpha \rho \zeta}{\lambda B(j, n+j+1)} \sum_{i=0}^{n-j} \sum_{j=l=0}^{\infty} (-1)^{i+k+l} {n-j \choose i} {i \choose k} (k+1)^{l} \zeta^{l+1}$$

$$\times \frac{x^{-\alpha-1} \left(1 + \frac{x^{-\alpha}}{\lambda}\right)^{-\rho(l+1)}}{(-e^{-\zeta} + 1)^{i+1} i!}$$
(33)

4. Estimation

Let $\underline{x} = x_1, x_2, ..., x_n$ represent a random sample of the *IPLP* distribution with unknown parameter vector $\Psi = (\alpha, \lambda, \rho, \zeta)$. The log likelihood $l = l(x, \Psi)$ for Ψ is

$$l(\underline{x}, \Psi) = log\left(\frac{\alpha\rho\zeta}{\lambda(-e^{-\zeta}+1)}\right) - (\alpha+1)\sum_{i=1}^{n}log(x_i) + (\rho+1)\sum_{i=1}^{n}log\left(1 + \frac{x^{-\alpha}}{\lambda}\right) \times -\zeta\sum_{i=1}^{n}\left(1 + \frac{x^{-\alpha}}{\lambda}\right)^{-\rho}$$
(34)

The score function $U(\Psi) = \left(\frac{\partial l}{\partial \alpha}, \frac{\partial l}{\partial \rho}, \frac{\partial l}{\partial \zeta}, \frac{\partial l}{\partial \lambda}\right)^T$ has components

$$\frac{\partial l}{\partial \alpha} = \frac{n}{\alpha} - \sum_{i=1}^{n} log(x_i)(\rho + 1) \sum_{i=1}^{n} \frac{x^{-\alpha}logx}{\lambda \left(1 + \frac{x^{-\alpha}}{\lambda}\right)} + \zeta \sum_{i=1}^{n} \rho \left(1 + \frac{x^{-\alpha}}{\lambda}\right)^{-\rho} x^{-\alpha}logx \quad (35)$$

$$\frac{\partial l}{\partial \rho} = \frac{n}{\rho} + \sum_{i=1}^{n} \log\left(1 + \frac{x^{-\alpha}}{\lambda}\right) + \zeta \sum_{i=1}^{n} \left(1 + \frac{x^{-\alpha}}{\lambda}\right)^{-\rho} \log\left(1 + \frac{x^{-\alpha}}{\lambda}\right)^{-\rho}$$
(36)

$$\frac{\partial l}{\partial \zeta} = \frac{n}{\zeta} - \frac{n}{(-e^{-\zeta} + 1)} - \sum_{i=1}^{n} \left(1 + \frac{x^{-\alpha}}{\lambda} \right)^{-\rho} \tag{37}$$

$$\frac{\partial l}{\partial \lambda} = -\frac{n}{\lambda} - (\rho + 1) \sum_{i=1}^{n} \frac{x^{-\alpha}}{\lambda^2 \left(1 + \frac{x^{-\alpha}}{\lambda}\right)} + \zeta \sum_{i=1}^{n} \frac{x^{-\alpha}}{\lambda^2 \left(1 + \frac{x^{-\alpha}}{\lambda}\right)}$$
(38)

The maximum likelihood estimate (MLE) $\widehat{\Psi}$ of Ψ is calculated numerically from the nonlinear equations $U(\Psi) = 0$. We use Adequacy Model in R to obtain $\widehat{\Psi}$.

4.1. Real data applications

In this section, we analyze two real data sets to demonstrate the flexibility and applicability of the proposed IPLP model. The first data set, representing strengths of 1.5 cm glass fibers, was previously studied by Smith and Naylor (1986). The second data set contain 40 times to failure of turbocharger of one type of engine and was previously studied by Al Sobhi (2022). The two data sets are carefully selected because they are negatively skewed and are either over- or under-dispersed. The IPLP model is compared to the one of the following competitive models: Inverse Lomax Poisson (ILP), Inverse Power Lomax (IPL), and Inverse Lomax models. In order to have a fair model comparison, we also use the following measures of goodness-of-fit criteria: Cramér Von-Mises (CVMS), Anderson-Darling (ADS), Kolmogorov-Smirnov (KSM), as well as those based on the log-likelihood: minus estimated -2*log-likelihood (-2l), Akaike information criterion (AICr), consistent Akaike information criterion (CAICr). The model with the minimum values for CVMS, ADS, KSM, AICr, and CAICr is considered to provide the best reasonable fits for the proposed data. Table 2 shows the exploratory data analysis for the two data sets which indicates that data I consist of 63 observations, negatively skewed, over-dispersed, with excess kurtosis of 0.92 that is leptokurtic. Data set II consist of 40 observations, under-dispersed, with excess kurtosis of -0.56 that is mesokurtic. Tables 3 and 5 gives the estimate of the parameters of the distributions considered.

Table 2. Exploratory data analysis of the two data sets

Specification	n	Min.	q_1	Median	q_3	mean	Max.	Var.	Kurt.	Skew.
Data I	63	0.55	1.38	1.59	1.69	1.51	2.24	0.11	3.92	-0.90
Data II	40	1.60	4.95	6.40	7.83	6.17	9.0	3.93	2.44	-0.55

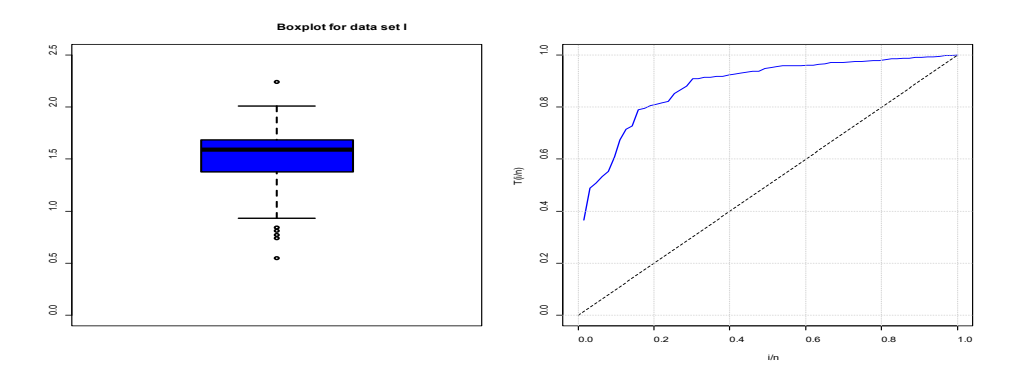


Figure 4. Box plot and the Total time on Test (TTT) plot for data set I

Figure 4 indicate that data set I is negatively skewed exhibiting an increasing failure rate.

Model	α	λ	ρ	ζ
IPLP	12.3939(0.7202)	0.0025(0.0007)	-2.7082(1.329)	0.2541(0.1010)
	{10.9823,13.8055}	{0.0011,0.0039}	$\{-5.3130, -1033\}$	{0.0561,0.4521}
ILP	_	0.3638(0.1939)	-2.2028(2.0980)	0.6170(0.3486)
	(-)	{-0.0162,0.7438}	{-6.3149,1.9093}	{-0.0663,1.3003}
IPL	11.5729(0.5958)	0.0021(0.0004)	0.4419(0.0615)	_
	{10.4051,12,7407}	{0.0013,0.0029}	{0.3214,0.5624}	(-)
IL	_	10.7375(5.8660)	15.5166(8.3418)	_
	(-)	{-0.7599,22.2349}	{-0.8333,31.8665}	(-)

Table 3. MLEs, their standard error (in parenthesis), confidence interval (curly) bracket for data set I

Table 4. Measures of goodness-of-fit value for data set I

Model	-2 <i>l</i>	AICr	BICr	HQICr	CAICr	KSN	ADS	CVMS	PV
IPLP	25.46	33.46	42.029	36.83	34.15	0.1188	0.8358	0.1521	0.3358
ILP	57.42	63.42	69.851	65.95	63.83	0.2364	3.2897	0.6001	0.0017
IPL	30.38	36.39	42.816	38.83	36.79	0.1643	1.3963	0.2534	0.0666
IL	182.48	186.48	190.76	188.16	186.68	0.4889	4.5411	0.8360	1.7e-13

From Table 4 it can be observed that the new developed inverse Power Lomax Poisson model has better fit than other three notable competitive models because it possessed the smallest value of the *AICr*, *CAICr*, *BICr*, *HQICr*, *KSM*, *ADS* and *CVMS* as well as largest *PV* value in modeling the glass fiber data.

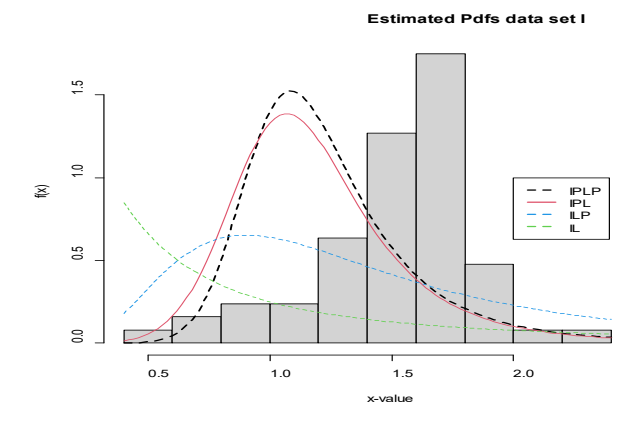


Figure 5. Graph of the fitted density for data set I

Figure 5 clearly indicates that *IPLP* model provides a better fit than all other models considered in the study.

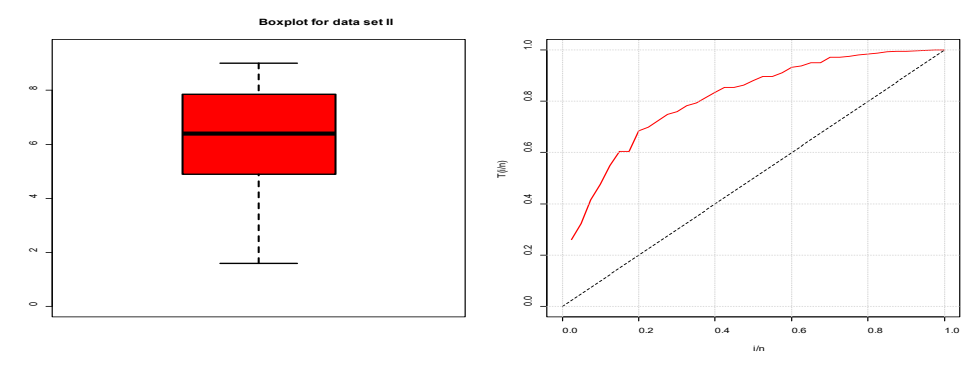


Figure 6. Box plot and the Total time on Test (TTT) plot for data set II

Figure 6 indicates that data set II is negatively skewed without any form of outlier exhibiting an increasing failure rate.

Table 5. MLEs, their standard error (in parenthesis), confidence interval (curly) bracket for data set II

Model	α	λ	ρ	ζ	
IPLP	1.8844(0.2453)	0.0077(0.0040)	29.9580(20.5404)	2.2498(0.3983)	
	{1.6391,2.3652}	$\{-0.0001, 0.0117\}$	{-10.3011,50.4984}	{1.4691,2.6481}	
ILP	_	10.4091(1.5213)	-9.8683(0.3210)	5.6043(1.2456)	
	(-)	{7.4274,11.9304}	{-10.4975, -9.2391}	{3.1629,8.0457}	
IPL	3.5615(0.2042)	0.0025(0.0006)	_	_	
	{3.1613,3.5615}	{0.0013,0.0031}	(-)	(-)	
IL	-	7.4952(8.9801)	39.5313(6.7337)	_	
	(-)	{-10.1058,25.0962}	{26.3333,52.7294}	(-)	

Table 6. Measures of goodness-of-fit value for data set II

Model	-2 <i>l</i>	AICr	BICr	CAICr	HQICr	KSM	ADS	CVMS	PV
IPLP	170.08	178.08	184.83	179.22	180.52	0.1038	0.7661	0.1069	0.7817
ILP	231.62	237.62	242.69	238.29	239.56	0.4346	2.0806	0.3355	5.5e-07
IPL	182.12	188.12	193.19	188.79	189.96	0.1756	1.5482	0.2406	0.1698
IL	288.66	232.67	236.04	232.99	233.89	0.4411	2.2521	0.3673	3.5e-07

From Table 6 it can be observed that the new developed Inverse Power Lomax Poisson model has better fit than other three notable competitive models because it possesses the smallest value of *AICr*, *CAICr*, *BICr*, *HQICr*, *KSM*, *ADS* and *CVMS* as well as the largest *PV* value in modeling the turbocharger data.

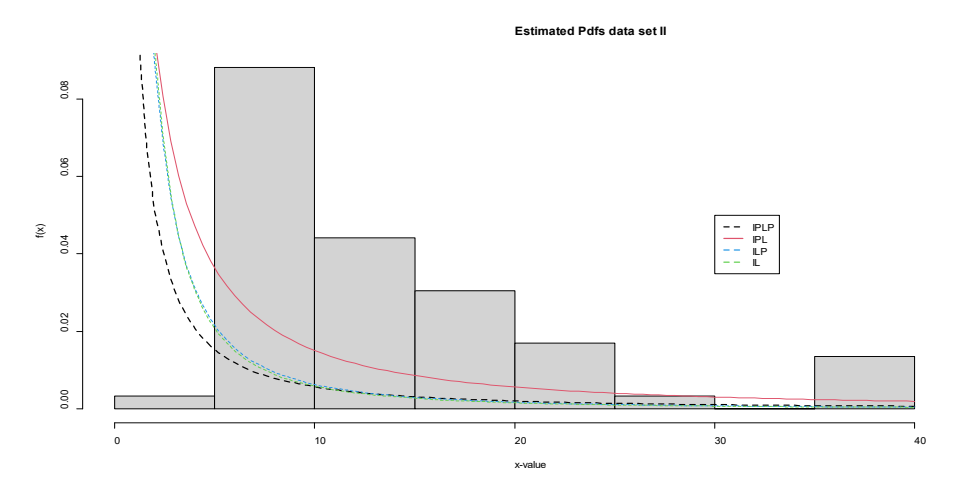


Figure 7. Graph of the fitted density for data set II

Figure 7 clearly indicates that *IPLP* model provides a better fit than all other models considered in the study.

Model	Hypothesis	LR	P – value			
IPLP vs ILP	H_0 : $\alpha = 1$ vs. H_1 : H_0 is false	31.96	< 0.001			
IPLP vs IPL	$H_0: \zeta = 1 \text{ vs. } H_1: H_0 \text{ is } false$	4.92	< 0.00			
IPLP vs IL	H_0 : $\alpha = \zeta = 1$ vs. H_1 : H_0 is false	157.02	< 0.001			
Data set II						
IPLP vs ILP	H_0 : $\alpha = 1 \text{ vs. } H_1$: H_0 is false	61.54	< 0.001			
IPLP vs IPL	$H_0: \zeta = 1 \text{ vs. } H_1: H_0 \text{ is } false$	12.04	< 0.001			
IPLP vs IL	H_0 : $\alpha = \zeta = 1$ vs. H_1 : H_0 is false	58.58	< 0.001			

Table 7. LR test for the two data sets

It can be observed from Table 7 that in each of the cases considered we accept the alternative hypothesis which is enough evidence that the *IPLP* model has a better fit than all other models considered for the two data sets and can effectively be used for fitting the data.

5. Concluding remarks

We have developed and studied the IPLP distribution along with its properties such as moments, incomplete moments, weighted moments, moment generating functions, Rènyi and q entropies, Bonferroni and Lorenz curves, reliability studies, stress-strength reliability and multi component stress-strength reliability model.

Maximum likelihood estimates are computed. Goodness-of-fit shows that the *IPLP* distribution is a better fit. Applications of the *IPLP* model to glass fiber and turbocharger data are presented to demonstrate its greater significance and better flexibility. We have shown that the *IPLP* distribution empirically provides reasonable fit for both the glass fiber and turbocharger data as supported by the graph of fitted densities and the likelihood ratio test statistics. In view of the shapes of the density and failure rate function, it can be concluded that the proposed model is a suitable candidate model in reliability analysis, data modeling, and other related fields. For future study, bivariate extension of the Inverse Power Lomax Poisson model can be considered.

Acknowledgement

We thank all the anonymous reviewers who have contributed to the final production of this article.

References

- Abd-Elfattah, A. M, Hassan, A. S. and Hussein, A. M., (2013). On the Lomax-Poisson Distribution. Proceeding of the 48th The Annual Conference On Statistics, Computer Sciences & Operations Research, Institute of Statistical Studies Research. *Cairo University*, pp. 25–39.
- Abdul-Moniem, I. B., Abdel-Hameed, H. F., (2012). A lifetime distribution with decreasing failure rate. *International Journal of Mathematical Education*, 33(5), pp. 1–7.
- Al-Marzouki, S., Jamal, F., Chesneau, C. and Elgarhy, M., (2020). Type II Topp Leone Power Lomax Distribution with Applications. Mathematics 2020, 8, 4, doi: 10.3390/math8010004.
- Al Sobhi, M. M., (2022). The extended Weibull distribution with its properties, estimation and modeling skewed data. *Journal of King Saud University Science*, 34(2), pp. 1–15.
- Al-Zahrani, B., (2015). An extended Poisson-Lomax distribution. *Advances in Mathematics: Scientific Journal*, 4(2), pp. 79–89.
- Al-Zahrani, B., Sagor, H., (2014). Statistical analysis of the Lomax-Logarithmic distribution. *Journal of Statistical Computation and Simulation*, 85, pp. 1883–1901.
- Cordeiro, G. M., Ortega. E. and Popović, B., (2013). The gamma-Lomax distribution. *Journal of Statistical Computation and Simulation*, 85(2), pp. 305–319.

- Haq, M. A., Hamedani, G. G., Elgarhy, M. and Ramos, P. L., (2020). Marshall-Olkin power Lomax Distribution: Properties and estimation based on complete and censored samples. *Int. J. Stat. Probab.*, 9(1), p. 48.
- Hassan, A. S.; Abd-Allah, M., (2019). On the Inverse Power Lomax Distribution. *Ann. Data Sci.*, 6, pp. 259–278, doi:10.1007/s40745-018-0183-y.
- Hassan, A. S., Nassr, S. G., (2018). Power Lomax Poisson distribution: Properties and Estimation. *Journal of Data Science*, 18, pp. 105–128.
- Lemonte, A. J., Cordeiro G. M., (2013). An extended Lomax distribution. *Statistics*, 47(4), pp. 800–816.
- Nagarjuma, V. B. V., Vardhan, R. V. and Chesnau, C., (2022). Nadarajah Haghighi-Lomax distribution and is Applications. *Math. Comput. Appl.*, 27 (30), pp. 1–13.
- Ramos, M. W. A., Marinho, P. R. D., da Silva R. V. and Cordeiro, G. M., (2013). The exponentiated Lomax Poisson distribution with an application to lifetime data. *Advances and Applications in Statistics*, 34(2), pp. 107–135.
- Roman, M., Louzada, F., Cancho, V. G. and Leite, J. G., (2012). A new long-term survival distribution for cancer data. *Journal of Data Science*, 10(2), pp. 241–258.
- Simth, R. L., Naylor, J. C., (1987). A comparison of maximum likelihood and Bayesian estimators for three-parameter Weibull distribution. *Applied Statistics*, 36, pp. 358–369.
- Tahir, M. H., Cordeiro, G. M., Mansoor, M. and Zubair, M., (2015). The Weibull-Lomax distribution: Properties and applications. *Hacettepe Journal of Mathematics and Statistics*, 44(2), pp. 461–480.
- Tahir, M. H., Hussain, M. A., Cordeiro, G. M., Hamedani, G. G., Mansoor, M. and Zubair, M., (2016). The Gumbel-Lomax distribution: Properties and applications. *Journal of Statistical Theory and Applications*, 15(1), pp. 61–79.